PERGAMON

International Journal of Heat and Mass Transfer 45 (2002) 381–391

International Journal of HEAT and MASS TRANSFER

www.elsevier.com/locate/ijhmt

Solution of inverse heat conduction problems using maximum entropy method

Sun Kyoung Kim, Woo Il Lee *

Department of Mechanical and Aerospace Engineering, San 56-1, Shinlim-dong, Kwanak-ku, Seoul 151-141, Republic of Korea

Received 25 October 2000; received in revised form 23 March 2001

Abstract

A solution scheme based on the maximum entropy method (MEM) for the solution of one-dimensional inverse heat conduction problem is proposed. The present work introduces MEM in order to build a robust formulation of the inverse problem. MEM finds the solution which maximizes the entropy functional under the given temperature measurements. In order to seek the most likely inverse solution, the present method converts the inverse problem to a non-linear constrained optimization problem. The constraint of the problem is the statistical consistency between the measured temperature and the estimated temperature. Successive quadratic programming (SQP) facilitates the maximum entropy estimation. The characteristic feature of the method is discussed with the sample numerical results. The presented results show considerable enhancement in the resolution of the inverse problem and bias reduction in comparison with the conventional methods.

1. Introduction

Inverse heat conduction problems (IHCP) aim to determine the unknowns such as thermal conditions [1,2], partially unknown geometry [3] and thermophysical properties [4] from known interior temperature history and distribution. Among such problems, the determination of surface heat flux has been investigated most extensively since it can be applied to a variety of real-world problems including aerodynamic heating during space vehicle reentry [5], quenching of metal under forced convection [6] and hyperthermia treatment [7].

Most difficulties in IHCPs are due to its extreme sensitivity to measurement errors, which incurs instability of the solution. In order to overcome such instability and to obtain a reliable inverse solution, a variety of numerical techniques have been proposed. These techniques include the least-squares method with regularization [1,8], the sequential function specification method (SFM) [1], space marching techniques [9–12], and the gradient method utilizing the adjoint problem [2]. A number of modifications to these methods have been made to enhance the solution behavior involving accuracy and stability. Despite such efforts, improvement in the resolution is limited by the conventional methods mentioned above. In some cases, the heat flux variation is so abrupt that the conventional methods lead to a meaningless inverse solution. Therefore, a stable way of enhancing the resolution and reducing the bias is essential for accurate recovery of the time-varying surface conditions with abrupt changes.

In this paper, the maximum entropy method (MEM) is introduced to IHCP to achieve the goal. MEM, which is based on the probabilistic theory, allows seeking the most likely inverse solution. MEM has been applied to various ill-posed problems including image reconstruction [13], ill-posed partial differential equation [14] and economic data recovery [15]. Generally, an inverse problem can be treated as an optimization problem. As for MEM, the consistency between the measurement and the estimation of temperature acts as a constraint of

* Corresponding author. Tel.: +82-2-880-7116; fax: +82-2-883-0179.

E-mail address: wilee@snu.ac.kr (W.I. Lee).

0017-9310/02/$ - see front matter
PII: S0017-9310(01)00155-7

Nomenclature

C_n	nth constraint
d	sensor location
f	unknown surface heat flux
f^e	original surface heat flux
$\mathbf{f}$	surface heat flux vector
f_0	a nominal heat flux
F	total sum of the heat flux components
H	entropy functional
J	residual functional
k	thermal conductivity
L	length of the domain
N	total number of heat flux components
N_d	number of subdivisions
NC	number of configurations
M	total number of spatial nodes
Pr	probability
r	random number
t	time
t_f	final time
T	computed temperature
T_0	initial temperature
x	distance from the heated surface
Y	measured temperature
α	thermal diffusivity
Δt	time interval
ε	convergence criterion
Λ_n	nth Lagrange multiplier
σ	standard deviation of the measured temperature

Subscripts

exact	exact data
i	index for heat flux component or time step index
m	configuration index
max	maximum

Superscript

+	non-dimensionalized

the optimization problem. The object functional of the optimization problem is the information entropy that is defined by Shannon [16]. Jaynes [17] proposed to use the information entropy in the field of statistical mechanics. By achieving the maximum state of the information entropy, uncertainty caused by the noise contained in the measurement data can be eliminated. MEM enables to obtain maximum possible information from given measurement data with limited accuracy. That is, if an inverse solution is a maximum entropy (ME) solution, it is the most likely solution among the candidates of many inverse solutions, which are consistent with the measurement data. This approach ensures the uniqueness of the inverse solution as well as the stability.

The entropy functional has a logarithmic form and the constraint has a quadratic form. Consequently, the solution procedure requires a non-linear constrained optimization. The non-linearity gives rise to computational difficulties. In the present study, the successive quadratic programming (SQP) is employed as a solution method for the optimization problem [20]. SQP is a general and straightforward method applicable for non-linear constrained optimization.

This work considers a typical one-dimensional IHCP. The reconstruction of a positive time-varying heat flux is conducted for varying measurement error levels and heat flux forms. Especially, impulse test is performed to investigate the deterministic characteristics of the scheme. The results of the proposed method based on MEM is compared with a conventional method in terms of the resolution and the bias of the solution.

2. Problem statement and governing equations

A finite one-dimensional slab with length L as illustrated in Fig. 1 is considered. The left side of the slab is exposed to unknown heat flux $f(t)$ and the right side is insulated. Material properties are considered constant over the entire domain. The measured temperature $Y(t)$ is acquired at a fixed location $x = d$. This problem is one of the most investigated inverse problems.

2.1. Direct problem

The governing equation for the one-dimensional heat conduction in a solid medium with constant material properties can be written as

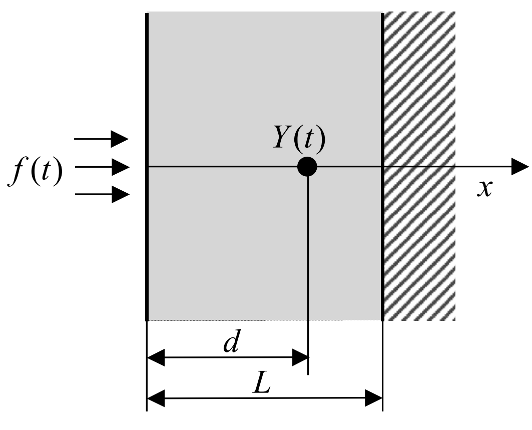

Fig. 1. One-dimensional domain considered in this study.

$$\frac{\partial T}{\partial t} = \alpha \frac{\partial^2 T}{\partial x^2} \quad 0 < x < L, \tag{1a}$$

where T is the temperature, α is the thermal diffusivity of the solid and x and t are the space and time variable, respectively. The corresponding initial condition is

$$T(x,0) = T_0(x), \tag{1b}$$

where $T_0(x)$ is the initial temperature distribution.

The boundary conditions are stated as

$$-k\frac{\partial T}{\partial x}\bigg|_{x=0} = f(t), \tag{1c}$$

where k is the thermal conductivity of the solid.

$$\frac{\partial T}{\partial x}\bigg|_{x=L} = 0. \tag{1d}$$

Direct solution of the problem gives temperature as a function of location and time for given initial and boundary conditions assuming the surface heat flux $f(t)$ as known. Thus, temperature for a particular function $f(t)$ can be denoted as $T(x,t;f)$.

2.2. Inverse problem

Through inverse analysis, the unknown condition which is consistent with temperature observation can be estimated. The temperature at $x = d$ is measured as a function of time $Y(t)$. If $Y(t)$ is free from measurement error, $f(t)$, which satisfies the expression

$$Y(t) = T(x,t;f) \tag{2}$$

can be the exact inverse solution. As is widely known, however, the direct imposition of Eq. (2) may result in erroneous and unstable oscillation since $f(t)$ is prone to measurement errors [1]. It is reasonable to select the following mean-square residual as a deviation measure for a sensor.

$$J(f) = \int_0^{t_f} [T(d,t;f) - Y(t)]^2 \, dt. \tag{3}$$

In general, $f(t)$ approaches the exact solution as $J(f)$ decreases. However, when $J(f)$ becomes smaller than a certain value, $f(t)$ starts to oscillate unexpectedly for noisy measurements. Therefore, a proper smoothing of the solution is essential. The degree of smoothing must be optimally controlled and proper criterion for the control needs to be established. If constant error level σ is assumed throughout the measurement, the following expression is admissible [2].

$$T(d,t;f) - Y(t) \cong \sigma, \tag{4}$$

where σ is the standard deviation of the temperature measurements. Then, the target value of the residual can be set as [2]

$$J(f) = \sigma^2 t_f, \tag{5}$$

where t_f is the final time for the measurement. Most practical inverse methods admit $f(t)$ approximately satisfying Eq. (5) as an inverse solution. Let us refer to such a solution as a feasible solution and refer to the above equality as a feasibility condition. A feasible solution is accepted as a solution that is statistically consistent with the measurement data. The regularization method (RM) with the least-squares method attempts to satisfy the condition via proper selection of the regularization parameter [8]. The sequential function specification method (SFM) controls the solution by a proper selection of the future time step and the function shape [1]. Instead, the conjugate gradient method (CGM) determines the solution by stopping the iteration on the condition that $J(f) \leqslant \sigma^2 t_f$, utilizing the viscous nature of the algorithm [2]. With the use of available means, each conventional method can achieve a feasible solution.

Despite the practical usefulness and wide acceptance of the conventional methods, the following problems concerning smoothing control and uniqueness of solution can be addressed. First, parameters such as the regularization parameter, the future time step and the number of iterations have loose relationships with physical nature and statistical uncertainty. The physical interpretations of these parameters in plain words are somewhat difficult and ambiguous. Thus, an approach that excludes additional parameters and reflects the uncertainty level directly on the inverse solution is more desirable. Second, as the solution obtained by the conventional methods depends on the path along which the solution is sought, the achieved solution varies according to the selection of the method for the identical temperature readings. In other words, the solution is not a unique one but just one of the admissible or feasible solutions. The conventional methods including RM, SFM, and CGM, can provide similar but different solutions for the identical IHCP. However, in terms of accuracy, the solution closer to the exact solution is preferred to other feasible solutions. A postulation can be made such that the unique solution exists among the feasible solutions which is statistically most likely for given measurement data [23]. Therefore, it is required to reformulate the inverse problem to determine the most likely solution. This study introduces the maximum entropy method (MEM) to IHCP to find such a solution. The way MEM achieves the most likely inverse solution and the manner in which MEM is implemented for IHCP are presented in the following section.

3. The maximum entropy formulation

As previously stated, the inverse problem is reformulated to seek the most likely solution among many feasible ones. In this study, MEM is adopted to serve the purpose. Firstly, the maximum entropy principle is introduced. The entropy functional which can measure the likelihood is defined. Secondly, the inverse problem is stated in the form of a non-linear constrained optimization. Most conventional inverse methods for IHCP can be regarded as unconstrained optimizations, which aim to achieve the feasibility condition only. On the other hand, the current optimization problem for MEM considers the entropy functional as an object. The feasibility condition given by Eq. (5) becomes a constraint. This feature enforces IHCP to be reformulated into a non-linear constrained optimization problem.

3.1. Maximum entropy principle

Consider N identical partitions as shown in Fig. 2. In the ith partition, a number of quantized heat fluxes, f_i, are stored. The total number of heat flux quanta F is

$$F = \sum_{i=1}^{N} f_i. \tag{6}$$

The value of F is to be known a priori with acceptable accuracy. The total number of ways of obtaining a particular configuration, denoted by NC, is given by [18]

$$NC(\mathbf{f}) = \frac{F!}{f_1!f_2!\dots f_N!}, \tag{7}$$

where $\mathbf{f} = \{f_1, f_2, \dots, f_N\}$.

For an arbitrary configuration $\mathbf{f}_m$ where m is an index which denotes a particular configuration, the probability of a specific configuration Pr is of the form

$$\Pr(\mathbf{f}_m) = \frac{NC(\mathbf{f}_m)}{\sum_m NC(\mathbf{f}_m)}. \tag{8}$$

If a configuration $\mathbf{f}_m$ makes the probability maximized, the configuration $\mathbf{f}_m$ can be accepted as the most probable or likely configuration. Because the denominator of the above expression is constant, $\Pr(\mathbf{f}_m)$ is maximized when $NC(\mathbf{f}_m)$ reaches the maximum. Removing the index m and applying Stirling's formula, we have [23]

$$NC(\mathbf{f}) \propto \exp\left[-\sum_{i=1}^{N} f_i \ln\frac{f_i}{F}\right]. \tag{9}$$

Here terms of lower order are neglected. Maximizing $NC(\mathbf{f})$ can be achieved by

$$\text{Maximize } H(\mathbf{f}) \equiv -\sum_{i=1}^{N} f_i \ln\frac{f_i}{F}. \tag{10}$$

Here H is called the information entropy [16]. Generally, the entropy in an isolated system never decreases, i.e., spontaneously tends towards the maximum value possible. In other words, since MEM reflects such property of nature, it searches the most natural solution rather than the smoothest solution. As a result, MEM enables us to minimize additional assumptions and information. On the contrary, the regularization method [8] needs careful selection of the regularization parameter, and the sequential function specification method [1] requires the number of future time steps and the functional form of f. In addition, MEM guarantees the uniqueness of the solution of ill-posed or even underdetermined inverse problems. Among the feasible solutions that satisfy the feasibility condition (Eq. (5)), the one that maximizes the entropy functional is accepted as the inverse solution. In this way, the uniqueness is guaranteed and the most likely solution can be obtained. A rigorous proof of the uniqueness is presented in the literature [18]. Above all, the most notable merit of MEM is that the enhancement of resolution and the suppression of noise are achieved at the same time. A detailed and comprehensive review of the characteristics of MEM can be found elsewhere [23].

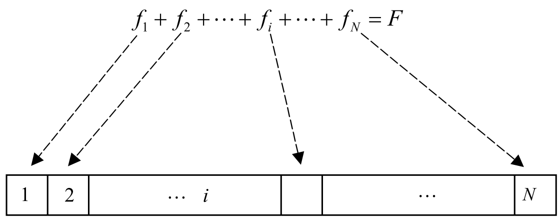

Fig. 2. Illustration of the partition and the distribution of heat flux quanta.

4. Optimization problem statement

If constant time interval is assumed, the following expression is valid:

$$t_f = N\Delta t, \tag{11}$$

where Δt is the constant time interval between each measurement. Generally, a non-linear equality like Eq. (5) is difficult to treat as a constraint. Hence, it is replaced by a tolerable criterion. The optimal control criterion is given by the following inequality [21]:

$$\left|J - N\sigma^2\Delta t\right| \leqslant \sqrt{2N}\sigma^2\Delta t. \tag{12}$$

The purpose here is to find the maximum entropy (ME) solution which maximizes H among feasible solutions. Therefore, the following statement can be made as an optimization problem:

Maximize the objective function $H(\mathbf{f})$

Subject to

Nonlinear equality constraint

$$C_1(\mathbf{f}) \equiv J - N\sigma^2\Delta t = 0 \tag{13}$$

with the maximum violation of $\sqrt{2N}\sigma^2\Delta t$,

Linear equality constraint

$$C_2(\mathbf{f}) \equiv \sum_{i=1}^{N} f_i - F = 0, \tag{14}$$

Bounds $\quad 0 < f_i \leqslant F. \qquad (15)$

Here the inequality constraint (Eq. (12)) is treated as an equality constraint of the optimization problem by setting $\sqrt{2N}\sigma^2\Delta t$ as the maximum violation of the equality constraint. The corresponding Lagrangian function can be written as

$$L = H - \Lambda_n C_n, \quad n = 1, 2, \tag{16}$$

where C_n denotes the constraints, and Λ_n is the Lagrange multiplier corresponding to each constraint. It is noted that the total sum F and the standard deviation σ are to be known a priori. In summary, MEM finds a unique distribution of the time varying heat flux with given F and σ under the assumption that the desired distribution is obtained via maximizing the entropy functional H. In order to perform the above optimization, a solution strategy must be carefully selected because of the nonlinear nature of H and J.

5. Solution procedure

The current approach requires more computational efforts compared to the conventional methods due to the requirement of the constrained optimization. Furthermore, the evaluation of the entropy functional requires the total sum F of the heat flux components f_i to be known a priori. In most cases, it is impractical to acquire the total sum in advance as provided data. In order to evaluate the total sum and provide the initial value for ME estimation, the conjugate gradient method (CGM) is utilized. CGM is based on the adjoint formulation which facilitates the evaluation of the gradient in an analytical manner [2]. The present method utilizes the adjoint formulation. Besides the evaluation of the total sum and the initial value, the gradient is also required for the ME estimation. It is provided by solving the adjoint problem which is solved to evaluate the gradients in CGM. In summary, the current approach is comprised of two computational phases. The first phase achieves a feasible solution by CGM. The second phase starts with the result of the first phase as an initial guess to estimate the ME solution. In the present study, the SQP is adopted to perform the optimization for the second phase.

5.1. First phase

A preliminary analysis is performed to provide the total sum and the initial guess for the ME estimation. Due to the energy conservation, the conventional inverse estimators for IHCP are capable of evaluating the total of the heat flux components ($F = \sum_{i=1}^{N} f_i$) with acceptable accuracy despite some local biases [19]. As stated earlier, CGM is used for the first phase. It is noted that the gradient is evaluated by solving the adjoint problem and the step size along the conjugate direction is determined utilizing the solution of the sensitivity problem without exhaustive line search. The adjoint formulation involving the adjoint problem and the sensitivity problem is already derived in complete and sound form by Alifanov for the one-dimensional case [2]. The procedure is not repeated here.

5.2. Second phase

In order to seek the solution of the prescribed nonlinear constrained optimization problem, the SQP is utilized [20]. SQP searches the desired optimum by repeating the following three steps consecutively: (i) approximation of the Lagrangian function in the quadratic form and the constraints in the linear form; (ii) determination of the search direction; (iii) control of the step length along the search direction with a proper penalty. SQP requires evaluation of the Hessian matrix and the gradient vector of H and J. The gradient vector of J can be obtained by solving the adjoint problem. The solution of the adjoint problem requires the estimated heat flux and the difference between the measured and the estimated temperatures. Both of them are available readily from the result of the previous iteration and the gradient can be easily evaluated during the optimization procedure. The Hessian matrix of J can be expressed as

$$\nabla\nabla J = \int_0^{t_f} \frac{\partial T}{\partial f_i}\frac{\partial T}{\partial f_j}\,\mathrm{d}t + \int_0^{t_f} \frac{\partial^2 T}{\partial f_i \partial f_j}[T(d,t;f) - Y(t)]\,\mathrm{d}t,$$
$$i = 1,\ldots,N,\ j = 1,\ldots,N. \tag{17}$$

The second integral term on the right-hand side is negligible since the second-order sensitivity $\partial^2 T/\partial f_i \partial f_j$ can be neglected for a linear IHCP (with constant thermophysical properties). As the first integral term forms a positive-definite matrix, $\nabla\nabla J$ can be regarded as positive-definite. However, it is not a simple task to evaluate $\nabla\nabla J$ directly in the adjoint formulation. In this work, $\nabla\nabla J$ is approximated by the Broyden–Fletcher–Goldfarb–Shanno (BFGS) update formula for computational efficiency and convergence [20]. Meanwhile, the evaluations of the gradient vector and the Hessian matrix of H are rather straightforward.

$$\nabla H = -\left(\ln\frac{f_i}{F} + 1\right), \quad i = 1,\ldots,N, \tag{18a}$$

$$\nabla\nabla H = -\frac{1}{f_i}\delta_{ij}, \quad i = 1,\ldots,N, \; j = 1,\ldots,N, \tag{18b}$$

where δ_{ij} is the Kronecker delta. The Hessian matrix of H is negative-definite and diagonal as shown above. As both Hessian matrices of the objective function and the non-linear constraint are sign-definite (i.e., convex), the global optimum can be achieved with uniform convergence [20]. Here the convergence is checked by the following criterion:

$$\frac{H^{k+1} - H^k}{H^k} < \varepsilon, \tag{19}$$

where k indicates the number of iterations and ε is chosen to be 10^{-3}. In this study, SQP is implemented by an existing computer code, CFSQP [25]. The code is slightly modified to allow $\nabla\nabla H$ to be provided by Eq. (18b) and to accommodate the above convergence criterion.

5.3. Discretization

Both phases require the numerical evaluation of temperature $T(x, t; f)$. This work adopts the finite volume method [22] with Crank–Nicolson scheme for the discretization in time and space. The spatial domain shown in Fig. 1 is discretized with M nodal points with equal spacing. In IHCP, the time step size for the discretization usually is identical to the measurement interval Δt. When the measurement interval is not sufficiently small, the solution may include considerable error due to incorrect integration in the time domain. In order to improve the accuracy, the time step is divided into a number of subdivisions. The number of subdivisions is defined as a preset number N_d. The estimated value of the heat flux and the measured data are available only at the discrete points. Accordingly, the linear interpolations are utilized for the intermediate points. This subdivision scheme is applied to the direct problem, the sensitivity problem and the adjoint problem at the same time.

6. Results and discussions

A few test cases are solved to verify the stability and accuracy of the proposed method. One-dimensional IHCP is investigated for different heat forms of heat fluxes, namely impulse and triangular heat flux. The heat fluxes estimated with MEM are compared with the original heat flux and the heat flux estimated with CGM.

6.1. Measurement data simulation

Test cases have been performed using measurement data artificially generated with and without errors. The errors are embedded to the exact data by the following equation:

$$Y_i = Y_{\text{exact}}, i + \sigma r_i, \quad i = 1,\ldots,N, \tag{20}$$

where r_i is a normally distributed random variable with zero mean and unit standard deviation. The random variable is generated by the IMSL® C function *random_normal* [26]. The exact data $Y_{\text{exact,i}}$ are obtained either by analytical or by numerical solution depending on the situations. The deterministic nature due to the numerical discretization error is investigated by comparing the recovered heat fluxes with the exact value obtained analytically or numerically. The necessity of the time step subdivision is also demonstrated for the impulse heat flux. The solution procedure for the exact data is presented elsewhere [1].

7. Definition of deviation measure and non-dimensionalized variables

In order to evaluate the bias of the inverse estimation, the following expression is chosen as a deviation measure:

$$D = \sqrt{\frac{1}{N-1}\sum_{i=1}^{N}(f_i - f_i^e)^2}, \tag{21}$$

where f_i^e is the ith heat flux component of the original heat flux.

The non-dimensionalized variables are defined as follows.

$$x^+ = x/L, \quad t^+ \equiv \frac{\alpha t}{L^2}, \quad \text{Fo}_d \equiv \frac{\alpha t}{d^2}, \tag{22a}$$

$$f^+ \equiv f/f_0, \quad T^+(x^+, t^+) \equiv \frac{T - T_0}{f_0 L/k}, \tag{22b}$$

where T_0 and f_0 are the nominal values of the temperature and the heat flux, respectively. Above non-dimensionalized values are used for presentation of the results. All the cases are tested under the identical condition $L = \alpha = k = f_0 = 1, T_0 = 0$ for simplicity. As a result, $x^+ = x, t^+ = t,\; f^+ = f$ and $T^+ = T$.

7.1. Verification with impulse heat flux

Raynaud and Beck suggested a dependable methodology of testing methods for IHCP [12]. In order to examine the trend of deterministic error, the test with impulse heat flux presented in the above work is applied to the proposed scheme. The impulse test is known to be the most stringent test of an IHCP algorithm. This test considers the recovery of the heat impulse which has non-zero, positive value only over a single time step (see Fig. 3). The impulse test is performed under the identical

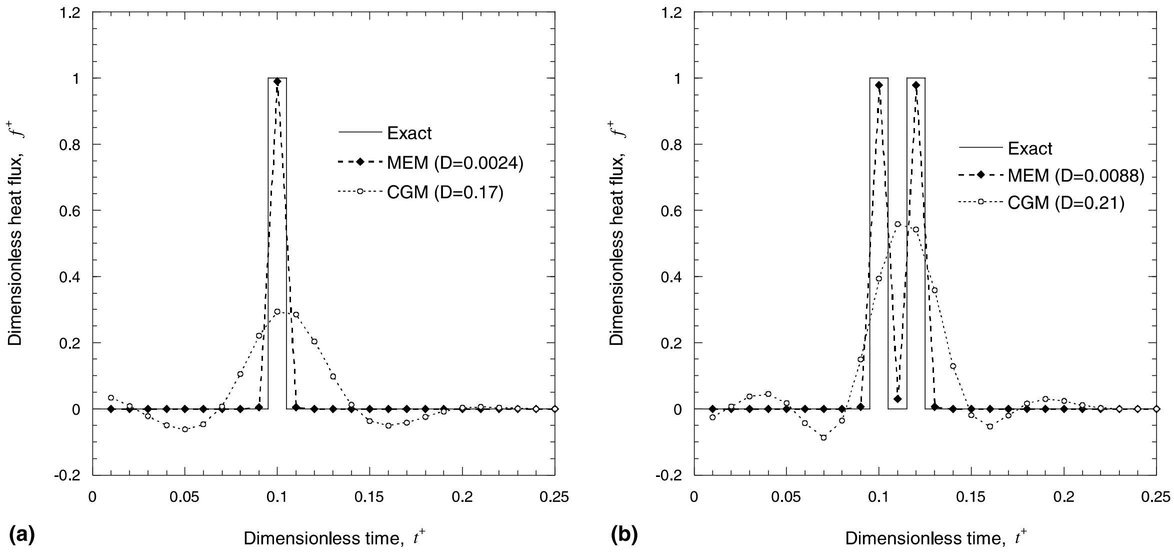

Fig. 3. Comparison of the heat flux estimated by MEM with the heat flux by CGM. Estimation performed with exact measurement data generated numerically for (a) single impulse and (b) two adjacent impulses.

condition suggested in the referenced work ($\Delta t = 0.01(\Delta Fo_d = 0.04)$, $t_f = 0.25$, $d = 0.5$ and $M = 21$). It is noted that the superposition of impulses of different strengths enables representing any time-varying heat flux. The impulse heat flux is given by (see Fig. 3)

$$f(t) = \begin{cases} 1, & 9.5\Delta t \leqslant t \leqslant 10.5\Delta t, \\ 0, & \text{elsewhere.} \end{cases} \tag{23}$$

The standard deviation σ is 0 for the exact measurement data. However, the smallest value of the residual functional J reachable by the present method is limited by errors induced by discretization, round-off and the number of significant digits of the measurement data. Therefore, whenever errorless data are used, σ is set equal to 10^{-5}.

Figs. 3(a) and (b) show the comparison between of the heat fluxes estimated by MEM and CGM. For this test run, the exact measurement data generated by the numerical calculation and the exact total sum are used. The result with CGM shows a smeared distribution centered on the impulse as shown in Fig. 3(a). The value of $\sqrt{J/(N\Delta t)}$ decreased to 3.7×10^{-4} in 25 (equal to N) iterations. However, ever after 500 iterations it could not be made smaller than 3.1×10^{-4}, which is required for estimating the presented result with CGM. On the contrary, the heat flux estimated by MEM shows nearly no bias, as can be seen in the figure. Such behavior of the inverse solution is known as super-resolution [24]. In order to test MEM for the more critical conditions, a test case with heat flux for two adjacent impulses is considered. The distance between each impulse is Δt.

Fig. 3(b) shows the comparison between the results by MEM and CGM for the two adjacent impulses. For results by MEM, two peaks are apparent without much smearing of the solution for the ME estimation as shown in the figure. On the contrary, the result by CGM exhibits a widely spread curve with single peak at the center of the two impulses. The resolution obtained by MEM is not possible by linear inversion techniques. The resolution of linear methods is restricted by the so-called Rayleigh limit [23].

As can be seen in the previous results, MEM can find a solution with nearly no deterministic error when the measurement data and the total sum are exact. If the total sum is not known a priori, the total sum has to be determined from a solution by CGM. Due to the energy conservation, the estimated value of the total sum can be approximated to the exact value. However, the estimated total sum may include an error to some extent. For example, the total sum of the solution with CGM shown in Fig. 3(a) is 0.983, where the exact value is equal to 1. Therefore, in order to investigate the effect of incorrect total sum, the impulse tests are done for $F = 0.5, 0.8, 0.9, 1.1$ and 2.0. Fig. 4 show the heat fluxes estimated using the corresponding value of the total sum. The numerically obtained data without error are generated for comparison. The underestimation of the total sum renders the peak location backward by as much as $2\Delta t$ for $F = 0.5$. For $F = 0.8$, amount of the backward shift is improved to Δt as shown in Fig. 4(a). Both the location and the peak value are not estimated properly for $F = 0.5$ and $F = 0.8$. However, in the case for $F = 0.9$, the peak location is accurately predicted. Therefore, it can be presumed that small amount of error in the total sum can be allowed and the total sum obtained using CGM is still valid for most ME

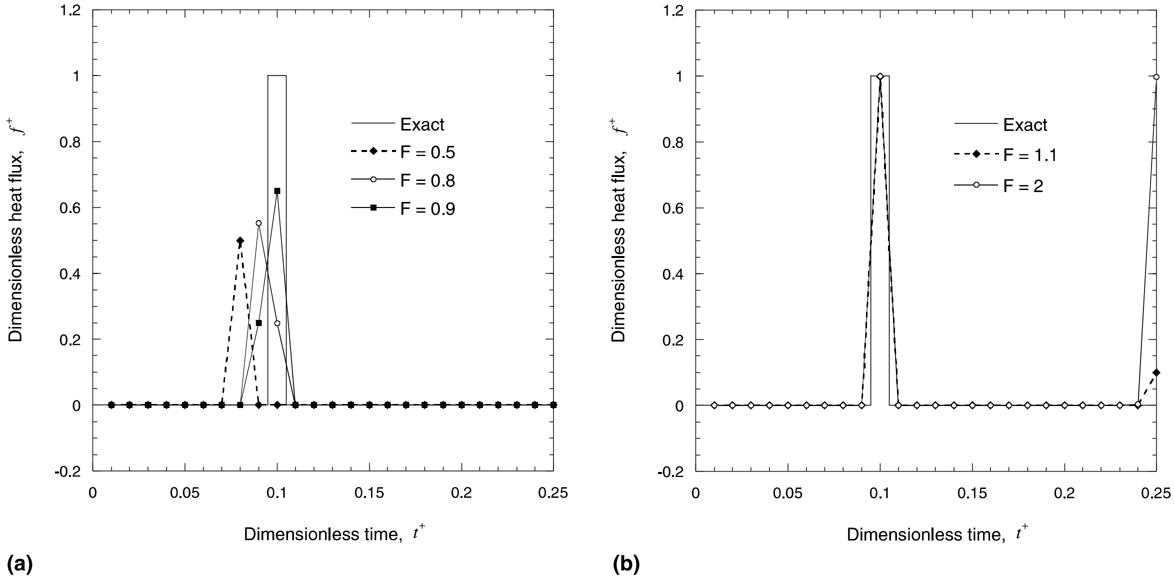

Fig. 4. Influence of inexact total sum on ME estimation with exact measurement data generated numerically for single impulse. Comparison between the exact heat flux and results using MEM: (a) for $F = 0.5$, 0.8 and 0.9; (b) for $F = 1.1$ and 2.0. Estimation performed.

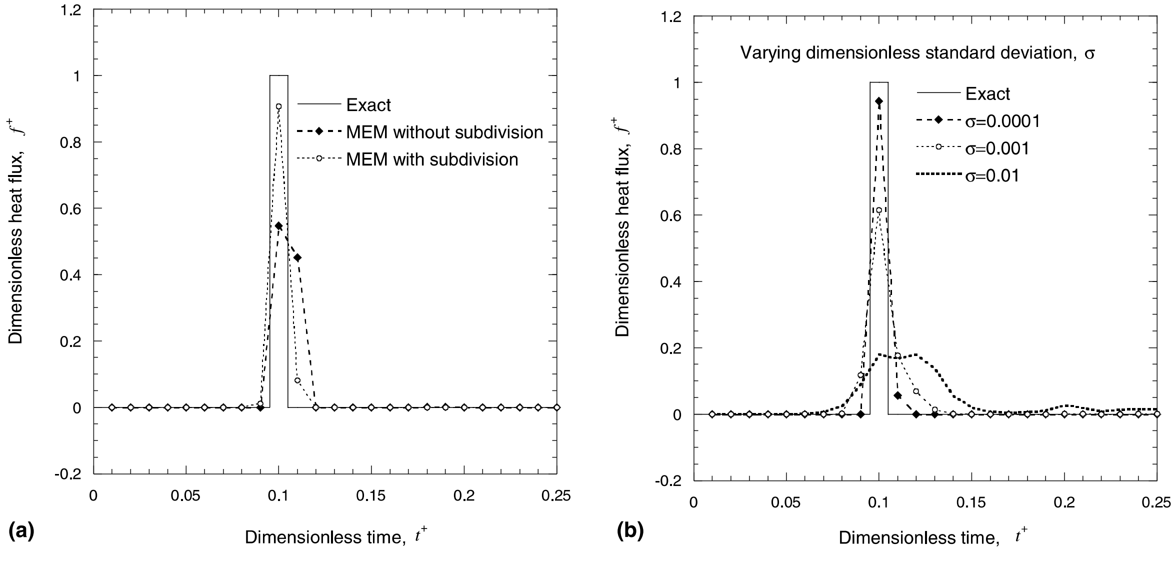

Fig. 5. Comparison of the heat fluxes estimated by MEM (a) with and without subdivision for $\sigma = 0$ and (b) with subdivision for $\sigma = 0.0001, 0.001$ and 0.01. Estimation performed with measurement data generated analytically for single impulse.

estimations. For values of F larger than unity, the peak locations are exact, as can be seen in Fig. 4(b). The amount added to the exact value of F augments only the least significant component f_N among the heat flux components. Because the heat flux component at the final time f_N has no effect on the measurement data, augmentation on f_N does not influence the residual functional J. Therefore, F values larger than 1 do not result in instability. It only brings about distortion of the solution.

Fig. 5(a) shows the heat flux estimated using the exact total sum and the exact measurement data from the analytic solution. The time step subdivisions of $N_d = 1$ and $N_d = 10$ are considered for this case, respectively. As can be seen in the figure, the estimated heat flux for $N_d = 1$ deviates considerably from the exact form due to coarse discretization used for the direct problem and the adjoint problem. On the other hand, such bias is nearly eliminated with more refined subdivision ($N_d = 10$). The subdivision technique is thought to be effective based on this example despite the possible inaccuracy caused by

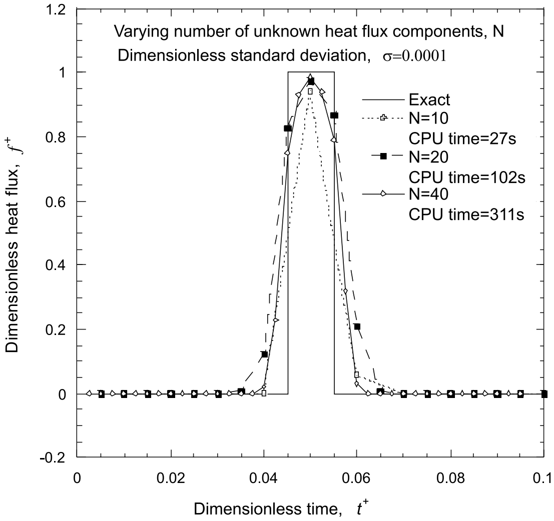

Fig. 6. Comparison of the heat fluxes estimated by MEM for different number of heat flux components N. Estimation performed with measurement data generated analytically for single impulse. Computations are performed on a PC equipped with Pentium processor.

the linear approximation. Therefore, it is possible that controlling stability by time step may yield inaccurate inverse solution.

The case with impulse heat flux is also considered in the presence of error in the measurement data. The measurement data are generated using the analytic solution. The error is embedded as was previously described. The time step subdivision of $N_d = 10$ is used. For the different error levels ($\sigma = 0.0001, 0.001$ and $0.01(\approx Y_{\max})$), the heat flux has been estimated. The results are shown in Fig. 5(b). Each curve exhibits acceptable results for different error levels. The heat flux estimated for $\sigma = 0.0001$ is nearly indistinguishable with the result shown in Fig. 5(a) which is recovered with the exact measurement data. In the case of $\sigma = 0.001$, clear peak is observed despite the presence of a noticeable error. The result is severely smeared for $\sigma = 0.01$ due to the extremely high disturbance in the measurement data. Although smeared, the result is thought to reveal the maximum information extractable from the disturbed data. As the increased error level enforces the inverse solution to be further ambiguous, additional information is necessary to resolve the ambiguity. Such information can be obtained via maximizing the entropy functional, and hence, the ME estimation can be used for measurement data with larger errors.

In order to investigate the effect of the number of unknown heat fluxes N on accuracy, an impulse test is performed. This test considers the ME estimation of the exact heat flux shown in Fig. 6 using noisy measurement data from the analytic solution. The parameters are $\sigma = 0.0001$, $N_d = 10$, $t_f = 0.1$. As N increases, the

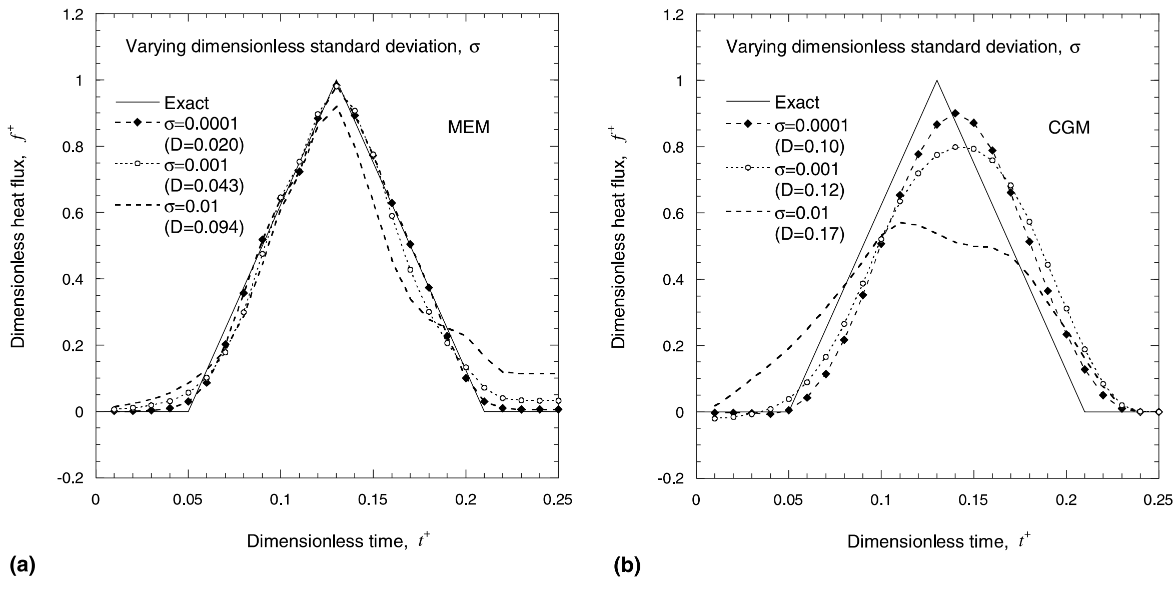

Fig. 7. Comparison of the heat fluxes estimated by (a) MEM and (b) CGM for different error levels σ. Estimation performed with measurement data generated analytically for triangular heat flux.

estimated heat flux becomes closer to the exact heat flux as can be seen in Fig. 6. At the same time, computational time increases drastically. Therefore, a proper trade-off between the accuracy and the cost has to be made.

7.2. Verification with triangular heat flux

Figs. 7(a) and (b) show the recovery of a triangular heat flux with MEM and CGM, respectively. The estimations have been conducted for $\sigma = 0.0001, 0.001$ and 0.01 with $N_d = 10$. The measurement data are generated analytically. All the heat fluxes reconstructed with MEM clearly show the apex at $t^+ = 0.13$ as can be seen in Fig. 7(a). Furthermore, the results for $\sigma = 0.0001$ and 0.001 agree quite well with the original heat flux in the entire domain. On the contrary, the heat fluxes recovered with CGM reveal considerable biases as shown in Fig. 7(b). Besides, smearing of the solution is observed. However, the difference between the deviation measures for MEM and CGM is greatly reduced in comparison with the difference for the impulse heat flux (see Fig. 3).

8. Concluding remarks

MEM is a non-linear inversion technique, which can enhance the resolution of the inverse estimation. The philosophy of MEM lies in seeking the most natural solution by accepting the principle of the spontaneous increase of entropy. MEM enables one to obtain the unique solution independent of the path and the method of optimization. The smoothing degree of inverse solution is controlled only by the error level of measurement data. It is independent of the optimization method [2] and can do without all other parameters like the number of future time steps [1] and the thermal wave speed [10] which may cause inevitable deterministic bias.

MEM is confined to positive heat flux reconstruction in nature. However, heat fluxes in many applications do not change sign in the entire time domain. The requirement of the total sum as a priori information can be satisfied by the preliminary estimation using CGM. If the accurate total sum is available, reliability of the estimation can be further improved. It is also noted that MEM calls for a lot of computational resources due to the non-linear constrained optimization. Although better resolution can be achieved apparently by increasing the number of unknowns N for the fixed time interval, N is to be determined considering the computational cost as shown in the result.

In this study, MEM is utilized for a linear one-dimensional IHCP. The results show reasonably good agreement with the exact heat flux. Whatever error level of the measurement might be, the proposed method is able to find the most statistically consistent result in a stable manner. A measure of improvement in resolution is achieved as can be observed in the presented results. The method is verified to be valid for quantitative accuracy enhancement of the heat flux recovery. MEM can be easily extended to other IHCPs and is expected to yield improved results.

Acknowledgements

This work was supported by the Brain Korea 21 Project and by Korean Ministry of Science and Technology through the National Lab Project.

References

[1] J.V. Beck, B. lackwell, C.R.S. Clair Jr., Inverse Heat Conduction, Wiley, New York, 1985.
[2] O.M. Alifanov, Inverse Heat Transfer Problem, Springer, Berlin, 1994.
[3] C.K. Hsieh, A.J. Kassab, A general method for the solution of inverse heat conduction problems with partially unkown geometries, Int. J. Heat Mass Transfer 29 (1) (1986) 47–58.
[4] G.P. Flach, M.N. Özişik, Inverse heat conduction problem of simultaneously estimating spatially varying thermal conductivity and heat capacity per unit volume, Numer. Heat Transfer Part A 16 (1989) 249–266.
[5] O.M. Alifanov, Mathematical and experimental simulation in aerospace system verification, Acta Astronautica 41 (1) (1997) 43–52.
[6] X.C. Huang, G. Bartsch, D. Schroeder-Richiter, Quenching experiments with a circular test section of medium thermal capacity under forced convection of water, Int. J. Heat Mass Transfer 37 (5) (1994) 803–818.
[7] C-T. Liauh, R.G. Hills, R.B. Roemer, Comparison of the adjoint and influence coefficient methods for solving the inverse hyperthermia problem, ASME J. Biomech. Eng. 115 (1993) 63–71.
[8] A.N. Tikhonov, V.Y. Arsenin, Soultion of Ill-posed Problems, Winstion & Sons, Washington, DC, 1977.
[9] N. D'Souza, Numerical soultion of one-dimensional inverse transient heat conduction by finite difference method, ASME Paper No. 75-WA/HT-81, 1975.
[10] C.F. Weber, Analysis and solution of the ill-posed inverse heat conduction problem, Int. J. Heat Mass Transfer 24 (1981) 1783–1792.
[11] E.C. Hensel, R.G. Hills, A apace marching finite difference algorithm for the one dimensional inverse heat conduction problem, ASME Paper No. 84-HT-48, 1984.
[12] M. Raynaud, J. Bransier, A new finite difference method for non-linear inverse heat conduction problem, Numer. Heat Transfer 9 (1) (1986) 27–42.
[13] J. Skilling, R.K. Bryan, Maximum entropy image reconstruction: general algorithm, Mon. Not. R. Astr. Soc. 211 (1984) 111–124.

[14] S. Ciulli, M. Mounsif, N. Gorman, T.D. Spearman, On the application of maximum-entropy to the moments problem, J. Math. Phys. 31 (1991) 1717–1719.
[15] A. Golan, G. Judge, Recovering information from incomplete or partial multisectoral economic data, Rev. Eco. Stat. 76 (1994) 541–549.
[16] C.E. Shannon, A mathematical theory of communication, Bell System Tech. J. 27 (1948) 379–423.
[17] E.T Jaynes, Information theory and statistical mechanics, Phys. Rev. 106 (1975) 620–630.
[18] H. Gzyl, The Method of Maximum Entropy, World Scientific, Singapore, 1995.
[19] M. Raynaud, J.V. Beck, Methodoloty for comparison of inverse heat conduction methods, ASME J. Heat Transfer 110 (1998) 30–37.
[20] G.V. Reklaitis, A. Ravindran, K.M. Ragsdell, Engineering Optimization, Wiley, New York, 1983.
[21] N.Y. Graham, Smoothing with periodic cubic splines, Bell System Tech. J. 62 (1983) 101–110.
[22] S.V. Patankar, Numerical Heat Transfer and Fluid Flow, Hemisphere, Washington, DC, 1980.
[23] N. Wu, The Maximum Entropy Method, Springer, Berlin, 1997.
[24] D.L. Donoho, I.M. Johnstone, J.C. Hoch, A.S. Stern, Maximum entropy and the nearly black object, J. R. Stat. Soc. B 54 (1) (1992) 41–81.
[25] C. Lawrence, Z.L. Zhou, A.L. Tits, User's Guide for CFSQP Version 2.5, Electrical Engineering Department and Institute for System Research, University of Maryland, 1997.
[26] IMSL® /C/Stat/Library™ User's Guide, Visual Numerics, 1998.